



Published in final edited form as:

Gastroenterology. 2015 October ; 149(4): 1030–1041.e6. doi:10.1053/j.gastro.2015.06.009.

Fat-specific Protein 27/CIDEA Promotes Development of Alcoholic Steatohepatitis in Mice and Humans

Ming-Jiang Xu^{1,2,*}, Yan Cai^{1,3,*}, Hua Wang^{1,4,*}, José Altamirano⁵, Binxia Chang¹, Adeline Bertola¹, Gemma Odena⁶, Jim Lu⁷, Naoki Tanaka³, Kimihiko Matsusue⁸, Tsutomu Matsubara³, Partha Mukhopadhyay⁹, Shioko Kimura³, Pal Pacher⁹, Frank J Gonzalez³, Ramon Bataller^{5,6,10}, and Bin Gao¹

¹Laboratory of Liver Diseases, National Institute on Alcohol Abuse and Alcoholism, National Institutes of Health, Bethesda, MD 20892, USA

²Department of Physiology and Pathophysiology, School of Basic Medical Science, Peking University, Beijing, China

³Laboratory of Metabolism, National Cancer Institute, National Institutes of Health, Bethesda, MD 20892, USA

⁴Department of Oncology, the First Affiliated Hospital of Anhui Medical University, Hefei, 230032, China

⁵Institut d'Investigacions Biomèdiques August Pi i Sunyer (IDIBAPS) and Liver Unit-Internal Medicine Department, Vall d'Hebron Hospital, Vall d'Hebron Institut de Recerca, Barcelona, Spain

⁶Department of Nutrition, University of North Carolina, Chapel Hill, Chapel Hill, NC 27599, USA

⁷GoPath Diagnostics, LLC, Chicago, IL 46240, USA

⁸Faculty of Pharmaceutical Science, Fukuoka University, Fukuoka, Japan

⁹Section on Oxidative Stress and Tissue Injury, Laboratory of Physiological Studies, National Institute on Alcohol Abuse and Alcoholism, National Institutes of Health, Bethesda, MD 20892, USA

¹⁰Department of Medicine, Division of Gastroenterology and Hepatology, University of North Carolina, Chapel Hill, NC 27599, USA

Corresponding authors: Bin Gao, M.D., Ph.D., Laboratory of Liver Diseases, NIAAA/NIH, 5625 Fishers Lane, Bethesda, MD 20892, USA; Tel.: 301-443-3998; bgao@mail.nih.gov.

*MJX, YC, and HW contributed equally to this work.

Publisher's Disclaimer: This is a PDF file of an unedited manuscript that has been accepted for publication. As a service to our customers we are providing this early version of the manuscript. The manuscript will undergo copyediting, typesetting, and review of the resulting proof before it is published in its final citable form. Please note that during the production process errors may be discovered which could affect the content, and all legal disclaimers that apply to the journal pertain.

Conflicts of interest: All authors disclose no conflicts.

MJX and YC designed and conducted mouse experiments and analyzed the results; HW designed and conducted the chronic-plus-multiple binge ethanol feeding model experiments; BC, AB, NT, KM, TM, PM, performed some mouse experiments and data analyses; JL analyzed liver pathology of mouse liver tissues; JTA, GO, and RB performed human AH sample studies and analyses; PP, SK, and FJG analyzed data and edited the manuscript; MJX and BG wrote the manuscript; BG designed the experiments and supervised the whole project.

Abstract

Background & Aims—Alcoholic steatohepatitis (ASH) is the progressive form of alcoholic liver disease and may lead to cirrhosis and hepatocellular carcinoma. We studied mouse models and human tissues to identify molecules associated with ASH progression, and focused on mouse fat-specific protein 27 (FSP-27)/human cell death-inducing DFF45-like effector C (CIDEDEC) protein, which is expressed in white adipose tissues and promotes formation of fat droplets.

Methods—C57BL/6N mice or mice with hepatocyte-specific disruption of *Fsp27* (*Fsp27*^{Hep-/-} mice) were fed the Lieber-Decarli ethanol liquid diet (5% ethanol) for 10 days to 12 weeks, followed by 1 or multiple binges of ethanol (5 or 6 g/kg) during the chronic feeding. Some mice were given an inhibitor of the peroxisome proliferator-activated receptor- γ (PPARG) (GW9662). Adenoviral vectors were used to express transgenes or small hairpin (sh) RNAs in cultured hepatocytes and in mice. Liver tissue samples were collected from ethanol-fed mice or from 31 patients with alcoholic hepatitis (AH) with biopsy-proved ASH and analyzed by histologic, immunohistochemical, transcriptome, immunoblot, and real-time PCR analyses.

Results—Chronic-plus-binge ethanol feeding of mice, which mimics the drinking pattern of patients with AH, produced severe ASH and mild fibrosis. Microarray analyses revealed similar alterations in expression of many hepatic genes in ethanol-fed mice and humans with ASH, including upregulation of mouse *Fsp27* (also called *Cidec*) and human *CIDEDEC*. *Fsp27*^{Hep-/-} mice and mice given injections of adenovirus-*Fsp27*shRNA had markedly reduced ASH following chronic-plus-binge ethanol feeding. Inhibition of PPARG and cyclic AMP-responsive element binding protein H (CREBH) prevented the increases in *Fsp27* α and *FSP27* β mRNAs, respectively, and reduced liver injury in this chronic-plus-binge ethanol feeding model. Overexpression of FSP27 and ethanol exposure had synergistic effects in inducing production of mitochondrial reactive oxygen species and damage to hepatocytes in mice. Hepatic *CIDEDEC* mRNA expression was increased in patients with AH and correlated with the degree of hepatic steatosis and disease severity including mortality.

Conclusion—In mice, chronic-plus-binge ethanol feeding induces ASH that mimics some histological and molecular features observed in patients with AH. Hepatic expression of FSP27/CIDEDEC is highly upregulated in mice following chronic-plus-binge ethanol feeding and in patients with AH; this upregulation contributes to alcohol-induced liver damage.

Keywords

lipid metabolism; endoplasmic reticulum; inflammation; translational research

Introduction

Excessive alcohol consumption is a leading cause of chronic liver diseases worldwide, causing a broad spectrum of illnesses, including steatosis, steatohepatitis (ASH), cirrhosis, and hepatocellular carcinoma.¹⁻³ Alcoholic hepatitis (AH), a severe form of alcoholic liver disease (ALD), can occur in patients with undergoing ALD and a history of recent excessive alcohol consumption, and it is associated with high mortality.⁴⁻⁸ The typical histology findings in AH patients show severe ASH, including steatosis, hepatocyte ballooning, neutrophilic infiltration, Mallory-Denk hyaline inclusions, and chicken wire fibrosis.⁴⁻⁸

Despite extensive research on ALD over the last 40 years, the pathogenesis of AH remains obscure and little progress has been made in the management of severe AH.^{4–9} Slow progress in the field of ALD has partly resulted from a lack of experimental models of advanced ALD and a lack of comparative translational studies. Many animal models have been used for the study of ALD, but few studies could reproduce the full spectrum of human AH.^{3, 10–12} Recently, a model of short-term (10-day)-plus-binge ethanol feeding in mice was developed,¹³ which showed significant elevation of serum ALT and AST, mild steatosis and neutrophil infiltration, but no liver fibrosis.¹³ Here, we extended the chronic ethanol feeding period to 8–12 weeks, followed by gavage of a single or multiple doses of ethanol. This model induced severe ASH and mild fibrosis.

To understand the pathogenesis of AH further, we developed an integrative approach by comparing transcriptome data from this clinically relevant model and biopsy-proven ASH from AH patients, and we identified many genes that were similarly dysregulated in the animal model and in AH samples. Among these genes, fat-specific protein 27 (*Fsp27*) and cell death-inducing DFF45-like effector C (*CIDE*C) were highly upregulated in this animal model and in AH samples, respectively. Mouse *Fsp27* gene is the human homologue of *CIDE*C, belonging to the family of CIDE proteins, which includes CIDEA, CIDEB, and CIDE C (human)/FSP27 (mice), and these proteins have been shown to play important roles in the development of metabolic disorders and nonalcoholic fatty liver disease (NAFLD) in addition to the regulation of cell apoptosis.^{14–17} FSP27 was found to be highly expressed in adipose tissues and to function as a lipid droplet-binding protein that promotes lipid accumulation in adipocytes.^{18, 19} While normal mouse livers express low levels of FSP27 protein, its expression is highly upregulated in NALFD,^{15, 20, 21} but not in chronic ethanol feeding-induced fatty liver.²¹ In the current study, we have demonstrated that hepatic expression of *Fsp27/CIDE*C is highly upregulated in chronic-plus-binge ethanol-fed mice and in human AH samples. Moreover, we provide evidence suggesting that FSP27/CIDE C promotes ASH in chronic-plus-binge ethanol-fed mice and in human AH.

Materials and Methods

Mice

Male mice were used in all experiments except the data in supporting Fig. 3. All of the animal experiments were approved by the NIAAA Animal Care and Use Committee.

Ethanol Feeding Protocols

Eight- to ten-week-old male mice were subjected to several different ethanol feeding protocols, including short-term or chronic-plus-one binge or multiple binges, chronic, or acute ethanol feeding. The details are described in supporting methods.

Human Liver Samples

Thirty-one consecutive AH patients admitted to the Liver Unit (Hospital Clinic, Barcelona, Spain) with biopsy-proven ASH were included. The details about these samples are described in supporting materials. The Ethics Committee of the Hospital Clinic approved the study protocol, and all of the patients provided written informed consent.

Other methods are described in supporting materials

Results

Chronic-plus-binge ethanol feeding induces more severe ASH than short-term-plus-binge feeding in mice

To characterize the chronic-plus-binge ethanol model, we evaluated the liver injury in male C57BL/6N mice fed ethanol for 10 days- to 12 weeks-plus-one binge, or for 8 weeks-plus-multiple binges of ethanol (two binges per week for 8 weeks).

As illustrated in Figs. 1A–B, the livers from chronically ethanol-fed mice (E8w) appeared pale, with mixed macro- and micro-steatosis; the range of steatosis was 5–20% (the percentage was calculated as the number of hepatocytes with obvious lipid droplets among the total number of hepatocytes). In contrast, the livers from mice chronically fed ethanol for 8–12 weeks-plus-one or multiple binges (E8w+1B, E12w+1B, E8w+nB) appeared very pale, with severe macrosteatosis as demonstrated by H&E staining. The range of steatosis was 20–80%.

Fig. 1C shows serum ALT and AST from different feeding models. Serum ALT levels were markedly elevated in chronic-plus-one binge-fed mice with the highest levels in E12w+1B and E8w+1B, followed by E4w+1B and E10d+1B groups. Interestingly, the serum AST levels were also markedly elevated in chronic-plus-binge ethanol-fed mice, but were comparable among these groups. In contrast, serum ALT and AST levels were slightly or not elevated in mice with pair feeding (P8w), with chronic ethanol feeding only (E10d, E8w, E12w), or with one or multiple binges only (1B, nB). Surprisingly, serum ALT and AST levels were lower in E8w+nB group compared to those in E8w+1B group (Fig. 1C). This may be due to the fact that E8w+1B represents acute-on-chronic liver injury while E8w+nB represents the mixture of acute-on-chronic and chronic liver injury model. The ongoing hepatocyte injury in E8w+nB was likely milder than that in E8w+1B at the time point when ALT and AST were measured. In addition, serum ALT and AST levels returned to basal levels 24 h post binge in the E8w+1B-treated mice; however, significant steatosis and neutrophil infiltration were still observed (supporting Fig. 1B).

We further characterized the chronic-plus-binge (E8w+1B and E8w+nB) models. As illustrated in Fig. 2 and supporting Fig. 2, the number of neutrophils, hepatic triglyceride levels, liver fibrosis (as determined by α -SMA staining, Sirius red staining, expression of collagens), the number of TUNEL⁺ hepatocytes were much greater in E8w+1B and E8w+nB groups than those in P8w or E8w groups. Surprisingly, the elevation of these parameters was similar in both E8w+1B and E8w+nB groups. Although the number of neutrophils was similar in these two groups, the infiltration pattern was very different. In E8w+1B group, neutrophils diffusely infiltrated the parenchyma while in E8w+nB group, many neutrophil clusters were observed (Fig. 2A–B and supporting Fig. 2A). In addition, hepatic levels of 4-hydroxynonenal (HNE) adducts and protein nitration were highly elevated in E8w+1B and E8w+nB groups compared to P8w or E8w groups, with significantly higher levels in the E8w+nB group than in the E8w+1B group (supporting Fig. 2). Finally, hepatic expression of several pro-inflammatory mediators were elevated in E8w

+1B and E8w+nB mice (Fig. 2C), with higher levels of *Cxcl4*, *Icam-1*, *Tnfa*, *IL-1 β* , *Ly6G* but lower levels of *Trail-r2*, *Tnfr1* in the latter group than those in the former group (the details about these factors are described in supporting materials).

Mallory-Denk bodies, which are formed by the accumulation of pre-keratin filaments in hepatocytes, are often observed in human AH.²² Although we did not observe Mallory-Denk bodies in this chronic-plus-binge model, keratin 8 and keratin 18, two major components of Mallory-Denk bodies,²² were upregulated by ~4–8 folds with much higher in E8w+nB than those in E8w+1B (supporting Fig. 2B).

Ballooning degeneration of hepatocytes is considered a hallmark of ASH and often accompanies necrotic damage.^{4, 5} Such ballooning hepatocytes were not observed in the chronic-plus-binge model; however, the number of TUNEL⁺ hepatocytes was markedly increased in this model, although there was no difference between E8w+1B and E8w+nB groups (Fig. 2A and supporting. 2B).

Finally, this chronic-plus-binge ethanol feeding model worked well in female C57BL/6N mice, inducing significant ASH (please see details in supporting materials and supporting Fig. 3).

Microarray analyses show that hepatic gene profiles in E8w+1B and E8w+nB mice are more similar than in E10d+1B mice to those in human AH

To further study the regulation of hepatic genes after chronic-plus-binge ethanol feeding, microarray analyses were performed from various groups. As shown in Supporting Figs. 4A–B, only 173 genes showed a >2-fold change in expression in E8w mice compared to pair-fed P8w mice (E8w vs. P8w), whereas 1253 genes showed a >2-fold change in expression in E8w+1B group relative to P8w group, which was much higher than the number of differentially regulated genes in E10d+1B group (825 genes) relative to P10d group. Microarray analyses of E8w+nB group revealed that the gene expression profiles from this group are very different from E8w+1B group, with much greater number of altered genes than those from E8w+1B group (supporting Figs. 4A–B).

To investigate the clinical relevance of this chronic-plus-binge ethanol model, we compared the gene expression profiles of these mice with those in human AH. As illustrated in supporting Fig. 4B, compared with human AH samples, E10d+1B, E8w+1B, and E8w+nB groups had 660, 1018, and 1225 genes that are similarly altered, respectively. Many of these differentially regulated genes were involved in lipid metabolism and hepatotoxicity (supporting Fig. 4C). The top 20 genes that were similarly altered in E8w+1B, E8w+nB, and human AH samples are listed in supporting Fig. 4D.

Chronic-plus-binge ethanol feeding upregulates hepatic Fsp27 α and Fsp27 β gene expression in mice in PPAR γ - and CREBH-dependent manner, respectively

Among the most highly upregulated genes, the *Fsp27* gene was upregulated by 13-fold and 4-fold in E8w+1B and E8w+nB group, respectively, and the expression of *CIDEA*, the human homologue of *Fsp27*, was upregulated by 5-fold in human AH (supporting Fig. 4D). Real-time PCR analyses confirmed that hepatic expression of *Fsp27* was elevated by 10-fold

after E8w+1B feeding, but only tend to increase without statistical significance after E10d +1B or single binge (1B) feeding (Fig. 3A). In contrast, hepatic *Cidea* and *Cideb* expression was not upregulated in E8w+1B group (Fig. 3B). Moreover, chronic ethanol feeding alone (E8w) did not alter hepatic *Cidea*, *Cideb*, or *Fsp27* gene expression (Fig. 3B).

Fsp27 gene exists two isoforms including *Fsp27 α* and *Fsp27 β* .²³ Here we also demonstrated that the livers from pair-fed (P8w) mice expressed both *Fsp27 α* and *Fsp27 β* mRNAs. The *Fsp27 β* mRNA is the predominant form that is 1000-fold higher than the *Fsp27 α* mRNA (Fig. 3C). Both isoforms were highly upregulated in E8w+1B and E8w+nB groups with greater elevation in the former group than the latter group (Fig. 3C). Elevation of FSP27 protein expression in E8w+1B mice was confirmed by western blot analysis (Fig. 3D).

Although E8w+1B feeding markedly upregulated hepatic expression of FSP27, incubation with up to 100 mM ethanol *in vitro* did not elevate FSP27 expression in primary hepatocytes (data not shown), suggesting ethanol does not directly upregulate hepatic FSP27 expression. *Fsp27* gene expression is controlled by several transcription factors, including cyclic-AMP-responsive-element binding protein H (CREBH),²³ PPAR γ ,¹⁵ and PPAR α .²⁴ Western blot analysis in Fig. 3D revealed that hepatic expression of PPAR γ and active nuclear form of CREBH-N protein was elevated after E8w+1B feeding, whereas PPAR α protein was slightly decreased. Additionally, hepatic expression of PPAR γ and CREBH-N protein was not altered after binge alone (supporting Fig. 5A).

CREBH is localized in the endoplasmic reticulum (ER) membrane and is activated by ER stress.²⁵ To examine whether activation of CREBH-N by E8w+1B feeding was due to activation of ER stress, hepatic expression of ER stress protein (the immunoglobulin-heavy-chain-binding protein [BiP]/78-kDa glucose-regulated protein [GRP78] and transcription factor C/EBP homologous protein [CHOP]) was measured. The results in Fig. 3D revealed that expression of both CHOP and BiP was significantly elevated in the E8w+1B-treated group, suggesting that E8w+1B feeding activates ER stress followed by activation of CREBH-N.

Finally, treatment of mice with the PPAR γ inhibitor GW9662 reduced the hepatic expression of *Fsp27 α* mRNA but not *Fsp27 β* mRNA in E8w+1B mice; while inhibition of hepatic CREBH expression by using Ad-shCREBH blocked *Fsp27 β* mRNA but not *Fsp27 α* mRNA (Figs. 3E–3F).

To examine whether upregulation of FSP27 conversely affects ER stress, we examined hepatic expression of ER stress proteins in *Fsp27* knockdown livers. As illustrated in supporting Fig. 5B, hepatic levels of BiP and CHOP as well as PPAR- γ and CREBH-N were not altered after *Fsp27* knockdown. Collectively, these results indicate that activation of ER stress upregulates hepatic *Fsp27* expression, while *Fsp27* does not affect ER stress gene expression.

Inhibition of *Fsp27* gene expression by injection of Ad-*Fsp27*shRNA or genetic disruption ameliorates chronic-plus-binge ethanol-induced ASH

To study the function of *Fsp27*, we used the Ad-*Fsp27*shRNA to suppress *Fsp27* expression or used hepatocyte-specific *Fsp27* knockout (*Fsp27*^{Hep-/-}) mice. As illustrated in Fig. 4 and supporting Fig. 6, E8w+1B or E8w+nB feeding-mediated induction elevation of serum ALT and AST, hepatic steatosis, and TUNEL⁺ hepatocytes were reduced in Ad-*Fsp27*shRNA-treated mice and *Fsp27*^{Hep-/-} mice compared to their corresponding controls. In addition, hepatic expression of several pro-inflammatory genes, fibrogenic genes, and keratin genes was lower in *Fsp27*^{Hep-/-} mice than in WT mice after E8w+nB treatment (Fig. 4F); however, expression of these genes was not reduced in *Fsp27*^{Hep-/-} and Ad-*Fsp27*shRNA-treated mice after E8w+1B challenge (supporting Figs. 7A–B). Interestingly, chronic ethanol feeding alone induced comparable levels of mild elevation of serum ALT and AST and hepatic triglyceride levels in *Fsp27*^{Hep-/-} and WT mice (supporting Fig. 8).

Moreover, treatment of mice with the PPAR γ inhibitor GW9662 or knockdown of *Crebh* by administration of Ad-sh*CREBH* partially ameliorated E8w+1B-induced elevation of serum ALT and AST levels, but did not reduce E8w+1B-induced elevation of hepatic pro-inflammatory mediators (Supporting Figs. 9A–D).

Ethanol and FSP27 synergistically promote mitochondrial reactive oxygen species (ROS) production in hepatocytes

Because induction of mitochondrial injury is an important mechanism underlying ethanol-induced liver injury,^{26, 27} we wondered whether FSP27 is involved in alcohol-induced hepatocyte mitochondria ROS production. As illustrated in Figs. 5A–5B, hepatic levels of malondialdehyde (MDA) and 4-HNE (oxidative stress/lipid peroxidation markers) were highly elevated in E8w+1B, and this elevation was attenuated after treatment with *Fsp27*shRNA. This suggests that FSP27 promotes ethanol-induced hepatic oxidative injury.

It is generally believed that FSP27 protein is located in cytoplasm and promotes fat lipid droplet formation.¹⁴ However, the function of FSP27 in mitochondria has not been examined. MitoProt II analysis²⁸ revealed that the FSP27 protein contains a sequence that is required for protein translocation into mitochondria, thus we asked whether FSP27 is located in mitochondria. To answer this question, we isolated cytoplasm and mitochondria from fresh liver tissues of E8w+1B-treated mice (those are known to express high levels of FSP27). Western blot analysis detected FSP27 protein in both cytoplasm and mitochondrial (Fig. 5C).

In addition, we overexpressed FSP27 protein in the liver or in primary hepatocytes via the treatment of Ad-*Fsp27*-HA (that contains a HA tag sequence). As illustrated in Fig. 5D and supporting Fig. 10A, anti-HA antibody detected the expression of FSP27-HA protein in both cytoplasm and mitochondria from the livers of mice infected with Ad-*Fsp27*-HA or in cultured *FSP27*-HA-transfected hepatocytes. Incubation with ethanol did not affect FSP27-HA expression in cultured hepatocytes (Fig. 5D). Moreover, overexpression of Ad-*Fsp27*-HA protein exacerbated the elevation of serum ALT and AST levels and decreased

mitochondrial contents and mitochondrial complex I activity in E8w+1B-treated mice (supporting Fig. 10B).

Next, we examined ROS production in cultured hepatocytes. As illustrated in Fig. 5E, hepatocytes from lean WT and *Fsp27*^{-/-} mice produced comparable levels of ROS post exposure to ethanol *in vitro*, suggesting that endogenous FSP27 has no effects on ROS production in normal hepatocytes. This may be due to the fact that normal hepatocytes express very low levels of endogenous FSP27 and incubation with ethanol does not upregulate FSP27 in hepatocytes (data not shown). Exposure to ethanol *in vitro* or overexpression of FSP27 itself increased mitochondrial ROS generation in hepatocytes. The combination of FSP27 overexpression and ethanol exposure synergistically increased mitochondrial ROS generation in hepatocytes (Fig. 5E). Finally, incubation with up to 600 mM ethanol did not cause death of Ad-control vector-treated hepatocytes, as measured by elevation of ALT, while as low as 100 mM ethanol caused death of Ad- *FSP27*-HA-treated hepatocytes (Fig. 5F).

To further examine the mechanism how FSP27 overexpression induces hepatocyte death in the presence of ethanol, we examined Bax translocation and cytochrome C release, two important early events in cell death. As illustrated in Fig. 5D, overexpression of *Fsp27* itself significantly induced Bax translocation to mitochondria and cytochrome C release, which were further exacerbated after incubation with ethanol.

Hepatic expression of *CIDEA* is increased in AH patients and correlated with disease severity

Microarray analysis revealed that *CIDEA* was upregulated by 5-fold in AH samples, compared with healthy control livers (supporting Fig. 4). Real-time PCR analysis of *CIDEA* mRNA was conducted in a cohort of patients with AH and revealed that hepatic expression of *CIDEA* mRNA was increased by more than 40-fold in AH samples but not in chronic hepatitis C or compensated cirrhosis samples (Fig. 6A). Moreover, hepatic *CIDEA* levels were higher in AH patients who had higher degrees of steatosis, and this expression was positively correlated with the prognostic MELD score and ABIC (age, serum bilirubin, INR, and serum creatinine) score²⁹ and with HVP (hepatic venous pressure gradient)³⁰ in AH patients (Figs. 6B–C). Importantly, hepatic levels of *CIDEA* mRNA were much higher in patients who died within 90 days after admission than in patients who survived (Fig. 6D). Finally, a Kaplan-Meier analysis was conducted to determine whether hepatic *CIDEA* mRNA expression was a good predictor of short-term mortality. As shown in Fig. 6E, hepatic *CIDEA* mRNA expression (receiver operating curve cut-off value of 37-fold ****[2□ Ct], AUROC 0.71, 95% CI [0.45–0.97]) was useful for predicting short-term mortality in AH patients. These findings suggest that *CIDEA* plays a role in promoting liver injury in AH and could be used as a biomarker to predict short-term mortality.

Discussion

In this paper, we developed a model of chronic-plus-binge ethanol feeding, which induced more severe ASH than short-term (10-day)-plus-binge model (the comparison of these models is summarized in supporting Table 3). By comparing transcriptome data from this

clinically relevant model with those from human ASH samples, we identified that FSP27/CIDEDEC was highly elevated and acted as an important mediator promoting ASH in chronic-plus-binge-fed mice and in human AH (Fig. 7).

Short-term-plus-binge vs chronic-plus-binge ethanol feeding

Compared with the shortterm E10d+1B model, the chronic E8w+1B and E8w+nB model induced more severe ASH and simulated some aspects of early steatohepatitis in AH patients, including elevation of serum ALT and AST levels, AST to ALT ratio >2, macrosteatosis, neutrophil infiltration, mild “chicken-wire” like fibrosis, and alterations in the expression of many genes related to lipid metabolism, hepatotoxicity, and inflammation. Although hepatic triglyceride levels, the number of neutrophils, and degree of liver fibrosis were comparable between E8w+1B and E8w+nB groups, there were some differences between the two groups described in supporting materials in detail.

In summary, E8w+1B and E8w+nB models represent a more advanced stage of ASH than E10d+1B model. While E8w+1B represents an acute-on-chronic liver injury, E8w+nB reproduces the mixture between chronic and acute-on-chronic liver injury models. Both E8w+1B and E8w+nB models still represent early stages of ASH. Recently, a complex hybrid model was developed by chronically feeding a high-fat, high-cholesterol, and ethanol diet to mice combined with gavage administration of ethanol.¹² This model simulates some features of severe AH. Thus, the E10d+1B, E8w+1B, E8w+nB, and the hybrid model may represent different stages of ASH.

Elevation of hepatic Fsp27/CIDEDEC in chronic-plus-binge-fed mice and human AH

By comparing the transcriptome data from E8w+1B and human AH samples, we identified 1018 genes that were similarly regulated between these two groups. Among them, hepatic *Fsp27* expression was highly elevated in E8w+1B-fed mice, and was also elevated in E8w+nB mice but to a lesser extent, however, its expression was only slightly elevated in E10d+1B and acute alcohol (1B)-fed mice, and not elevated in chronic ethanol-fed mice (this study and reference²¹). Hepatic expression of *CIDEDEC* was also upregulated in human AH but not in alcoholic cirrhotic livers or chronic HCV-infected livers. Collectively, these findings suggest that hepatic *Fsp27/CIDEDEC* is highly elevated in acute-on-chronic alcoholic liver injury (E8w+1B and human AH), and this elevation is less obvious in E8w+nB (a model mimicking mixture of acute-on-chronic and chronic) and not elevated in E8w (chronic injury).

The next question concerned the cause of *Fsp27/CIDEDEC* upregulation in E8w+1B mice and human AH. It has been well documented that hepatic expression of *Fsp27* is controlled by CREBH,²³ PPAR γ ,¹⁵ and PPAR α .²⁴ Both CREBH and PPAR γ were upregulated in the liver after E8w+1B treatment, and blockage of them ameliorated hepatic expression *Fsp27*. This suggests that chronic-plus-binge ethanol feeding upregulates hepatic *Fsp27* expression via the activation of CREBH-N and PPAR γ . In addition, we found that E8w+1B treatment markedly activated hepatic ER-stress protein CHOP and Bip. Although we did not examine the link between this ER stress and *FSP27* upregulation, several recent studies reported that activation of ER stress by various stimuli upregulated PPAR- γ , CREBH-N, and *FSP27* in

hepatocytes.^{25, 31} Thus it is plausible that activation of ER stress by E8w+1B contributes to the hepatic FSP27 upregulation in this model via the activation of PPAR- γ and CREBH-N.

PPAR γ expression was elevated after E8w+1B challenge, and treatment with a PPAR γ antagonist partially reduced hepatic expression of *Fsp27a* mRNA and ameliorated elevation of serum ALT and AST. PPAR γ was shown to promote hepatic steatosis^{32, 33} but to inhibit inflammation³⁴ in NAFLD, and the anti-inflammatory effect is mediated by its primary insulin-sensitizing effect on adipose tissue.³⁴ In contrast to NAFLD, the alcohol feeding model is only associated with hepatic steatosis but not obesity. Thus, PPAR γ likely exerts a predominant pro-steatotic effect in chronic-plus-binge ethanol feeding model, and inhibition of PPAR γ by an antagonist shows beneficial effects by ameliorating alcoholic liver injury. In addition, the pro-steatotic effect of PPAR γ in hepatocytes is mediated via the upregulation of *Fsp27* gene.^{32, 33} However, because FSP27 α is a very minor form in the liver, which is 1000-fold lower than FSP27 β expression, the downregulation of FSP27 α by GW9662 may not or only partially account for the protective effect of the PPAR γ antagonist GW9662 treatment in the E8w+1B model. There may be other factors, but yet not clear, also contribute to the amelioration of liver injury in E8w+1B mice by GW9662 treatment.

An important role of FSP27/CIDEc in acute-on-chronic ethanol-induced liver injury and human AH

Genetic deletion of hepatic *Fsp27* gene markedly ameliorated chronic-plus-binge ethanol-induced liver injury but not chronic ethanol-induced liver injury, suggesting that FSP27 promotes ASH induced by chronic-plus-binge ethanol feeding but not by chronic ethanol feeding. The mechanisms by which FSP27 induces fat droplet formation have been extensively studied;¹⁴ however, how FSP27 promotes cell injury is poorly understood. One mechanism underlying FSP27-mediated liver injury is the induction of steatosis and subsequent lipotoxicity. In addition, in this study, we demonstrated that FSP27 is also located in hepatocyte mitochondria and together with ethanol exposure synergistically induce mitochondrial ROS production and subsequent hepatocyte death. Thus, direct induction of mitochondrial ROS production is another important mechanism by which FSP27 promotes alcoholic liver injury. Furthermore, we show that overexpression of FSP27 inhibits mitochondrial complex I activity in the liver, which likely contributes to FSP27-mediated induction of ROS in mitochondria.

CIDEc, the human homolog of FSP27, is mainly expressed in white adipose tissues, and has been shown to promote fat droplet formation and cell apoptosis in adipocytes.^{14, 16} CIDEc is expressed at low levels in normal healthy human livers, but is markedly upregulated in NAFLD.²⁰ However, the functions of CIDEc in the pathogenesis of human liver diseases have not been explored. In the current paper, we demonstrated that *CIDEc* mRNA was upregulated by approximately 40-fold in human AH compared with normal healthy controls. Although we demonstrated that hepatic FSP27 is highly elevated in severe AH, whether hepatic FSP27 is also upregulated in patients with milder forms of ASH or fatty liver deserves further investigation.

The upregulation of *CIDEc* mRNA was positively correlated with the degree of hepatic steatosis, the severity of disease, and the mortality of AH patients. Because knockdown of

FSP27 ameliorates chronic-plus-binge ethanol-induced ASH in mice, we speculate that upregulation of CIDEC contributes to the pathogenesis in AH patients by promoting steatosis and hepatocyte damage, and subsequently inducing neutrophilic infiltration.

Roles of FSP27 in E8w+1B and E8w+nB-induced liver injury

Hepatic FSP27 was upregulated in both E8w+1B and E8w+nB models with much higher levels in E8w+1B than in E8w+nB. Knockdown of FSP27 ameliorated the elevation of serum ALT and AST, and steatosis in both models. However, genetic disruption of the *Fsp27* gene reduced expression of inflammatory genes and collagens in E8w+nB model but not in E8w+1B model. This indicates that the wound healing response in E8w+nB and E8w+1B models is FSP27-dependent and -independent, respectively (Fig. 7). E8w+1B represents an acute-on-chronic liver injury model, in which hepatic FSP27 is only markedly upregulated post 1B treatment in the chronic (8w) ethanol-fed mice. This transient FSP27 elevation likely induces steatosis and liver injury but not inflammation and fibrosis in E8w+1B model. In contrast, E8w+nB represents a mixture of chronic and acute-on-chronic liver injury, in which hepatic FSP27 elevation is prolonged. This sustained FSP27 expression in hepatocytes likely causes the chronic liver injury and inflammation, and may subsequently induce fibrosis in E8w+nB model (Fig. 7).

Although genetic disruption of the *Fsp27* gene in hepatocytes did not affect hepatic collagen expression in E8w+1B model, inhibition of *Fsp27* by administration of adeno-sh*Fsp27* enhanced hepatic collagen expression (supporting Fig. 7). It is plausible that injection of adeno-sh*Fsp27* downregulates *Fsp27* expression not only in hepatocytes but also in stellate cells, and that elevated hepatic collagen expression by Ad-sh*Fsp27* was due to inhibition of *Fsp27* in stellate cells. In fact, FSP27 can directly inhibit stellate cell activation and liver fibrosis.³⁵

Conclusion: in the current study, we developed an integrative biological approach by analyzing transcriptome data from chronic-plus-binge ethanol-fed mice and human AH, and we demonstrated that FSP27/CIDEC plays important roles in promoting ASH in this mouse model and in AH patients. This approach could be used in the future to identify and investigate other important mediators that may contribute to the pathogenesis of ASH, and it will likely facilitate the discovery of novel therapeutic targets for the treatment of this severe clinical condition.

Supplementary Material

Refer to Web version on PubMed Central for supplementary material.

Acknowledgments

The authors would like to thank Dr. Kezhong Zhang (The Wayne State University School of Medicine, Detroit, MI) for kindly providing us the plasmids of shCREBH, and also thank Huan Xu for her generous help on mouse ethanol feeding.

This work was supported by the intramural program of the NIAAA, NIH (B. Gao), 1U01AA021908-01 (RB), and the National Natural Science Foundation of China (81470557) and the National Basic Research Program of China (2012CB518002) (MJ Xu).

Abbreviations

ABIC	age, serum bilirubin, INR, and serum creatinine score
AH	alcoholic hepatitis
ALD	alcoholic liver disease
ASH	alcoholic steatohepatitis
BiP	immunoglobulin-heavy-chain-binding protein (BiP)
CHOP	transcription factor C/EBP homologous protein
CIDE-C	cell death-inducing DFF45-like effector C
CREBH	cyclic-AMP-responsive- element binding protein H
E10d+1B	short-term (10 days) plus single binge ethanol feeding
E4W+1B, E8w+1B, and E12W+1B	long-term (4, 8 and 12 weeks) plus single binge ethanol feeding, respectively
E8w+nB	long-term (8 weeks) plus multiple binges of ethanol feeding
FSP27	fat-specific protein 27
GRP78	78-kDa glucose-regulated protein
HVPG	hepatic venous pressure gradient
PPARγ	peroxisome proliferator-activated receptor γ
ROS	reactive oxygen species.

References

1. Gao B, Bataller R. Alcoholic liver disease: pathogenesis and new therapeutic targets. *Gastroenterology*. 2011; 141:1572–1585. [PubMed: 21920463]
2. Tsukamoto H, Lu SC. Current concepts in the pathogenesis of alcoholic liver injury. *FASEB J*. 2001; 15:1335–1349. [PubMed: 11387231]
3. Williams JA, Manley S, Ding WX. New advances in molecular mechanisms and emerging therapeutic targets in alcoholic liver diseases. *World J Gastroenterol*. 2014; 20:12908–12933. [PubMed: 25278688]
4. Lucey MR, Mathurin P, Morgan TR. Alcoholic hepatitis. *N Engl J Med*. 2009; 360:2758–2769. [PubMed: 19553649]
5. Singal AK, Kamath PS, Gores GJ, et al. Alcoholic hepatitis: current challenges and future directions. *Clin Gastroenterol Hepatol*. 2014; 12:555–564. quiz e31–2. [PubMed: 23811249]
6. Mathurin P, Lucey MR. Management of alcoholic hepatitis. *J Hepatol*. 2012; 56(Suppl 1):S39–S45. [PubMed: 22300464]
7. Altamirano J, Bataller R. Alcoholic liver disease: pathogenesis and new targets for therapy. *Nat Rev Gastroenterol Hepatol*. 2011; 8:491–501. [PubMed: 21826088]
8. Chayanupatkul M, Liangpunsakul S. Alcoholic hepatitis: a comprehensive review of pathogenesis and treatment. *World J Gastroenterol*. 2014; 20:6279–6286. [PubMed: 24876748]
9. Thursz MR, Richardson P, Allison M, et al. Prednisolone or pentoxifylline for alcoholic hepatitis. *N Engl J Med*. 2015; 372:1619–1628. [PubMed: 25901427]
10. Brandon-Warner E, Schrum LW, Schmidt CM, et al. Rodent models of alcoholic liver disease: Of mice and men. *Alcohol*. 2012; 46:715–725. [PubMed: 22960051]

11. Ueno A, Lazaro R, Wang PY, et al. Mouse intragastric infusion (iG) model. *Nat Protoc.* 2012; 7:771–781. [PubMed: 22461066]
12. Lazaro R, Wu R, Lee S, et al. Osteopontin deficiency does not prevent but promotes alcoholic neutrophilic hepatitis in mice. *Hepatology.* 2015; 61:129–140. [PubMed: 25132354]
13. Bertola A, Mathews S, Ki SH, et al. Mouse model of chronic and binge ethanol feeding (the NIAAA model). *Nat Protoc.* 2013; 8:627–637. [PubMed: 23449255]
14. Xu L, Zhou L, Li P. CIDE proteins and lipid metabolism. *Arterioscler Thromb Vasc Biol.* 2012; 32:1094–1098. [PubMed: 22517368]
15. Matsusue K, Kusakabe T, Noguchi T, et al. Hepatic steatosis in leptin-deficient mice is promoted by the PPAR γ target gene *Fsp27*. *Cell Metab.* 2008; 7:302–311. [PubMed: 18396136]
16. Yonezawa T, Kurata R, Kimura M, et al. Which CIDE are you on? Apoptosis and energy metabolism. *Mol Biosyst.* 2011; 7:91–100. [PubMed: 20967381]
17. Gong J, Sun Z, Li P. CIDE proteins and metabolic disorders. *Curr Opin Lipidol.* 2009; 20:121–126. [PubMed: 19276890]
18. Puri V, Konda S, Ranjit S, et al. Fat-specific protein 27, a novel lipid droplet protein that enhances triglyceride storage. *J Biol Chem.* 2007; 282:34213–34218. [PubMed: 17884815]
19. Nishino N, Tamori Y, Tateya S, et al. FSP27 contributes to efficient energy storage in murine white adipocytes by promoting the formation of unilocular lipid droplets. *J Clin Invest.* 2008; 118:2808–2821. [PubMed: 18654663]
20. Hall AM, Brunt EM, Klein S, et al. Hepatic expression of cell death-inducing DFFA-like effector C in obese subjects is reduced by marked weight loss. *Obesity (Silver Spring).* 2010; 18:417–419. [PubMed: 19661960]
21. Aibara D, Matsusue K, Matsuo K, et al. Expression of hepatic fat-specific protein 27 depends on the specific etiology of fatty liver. *Biol Pharm Bull.* 2013; 36:1766–1772. [PubMed: 24189421]
22. Zatloukal K, French SW, Stumpfner C, et al. From Mallory to Mallory-Denk bodies: what, how and why? *Exp Cell Res.* 2007; 313:2033–2049. [PubMed: 17531973]
23. Xu X, Park JG, So JS, et al. Transcriptional activation of *Fsp27* by the liver-enriched transcription factor CREBH promotes lipid droplet growth and hepatic steatosis. *Hepatology.* 2015; 61:857–869. [PubMed: 25125366]
24. Langhi C, Baldan A. CIDE/CSP27 is regulated by peroxisome proliferator-activated receptor α and plays a critical role in fasting- and diet-induced hepatosteatosis. *Hepatology.* 2015; 61:1227–1238. [PubMed: 25418138]
25. Zhang K, Shen X, Wu J, et al. Endoplasmic reticulum stress activates cleavage of CREBH to induce a systemic inflammatory response. *Cell.* 2006; 124:587–599. [PubMed: 16469704]
26. Hoek JB, Cahill A, Pastorino JG. Alcohol and mitochondria: a dysfunctional relationship. *Gastroenterology.* 2002; 122:2049–2063. [PubMed: 12055609]
27. Chacko BK, Srivastava A, Johnson MS, et al. Mitochondria-targeted ubiquinone (MitoQ) decreases ethanol-dependent micro and macro hepatosteatosis. *Hepatology.* 2011; 54:153–163. [PubMed: 21520201]
28. Claros MG, Vincens P. Computational method to predict mitochondrially imported proteins and their targeting sequences. *Eur J Biochem.* 1996; 241:779–786. [PubMed: 8944766]
29. Dominguez M, Rincon D, Abraldes JG, et al. A new scoring system for prognostic stratification of patients with alcoholic hepatitis. *Am J Gastroenterol.* 2008; 103:2747–2756. [PubMed: 18721242]
30. Bosch J, Abraldes JG, Berzigotti A, et al. The clinical use of HVPG measurements in chronic liver disease. *Nat Rev Gastroenterol Hepatol.* 2009; 6:573–582. [PubMed: 19724251]
31. Lee JS, Mendez R, Heng HH, et al. Pharmacological ER stress promotes hepatic lipogenesis and lipid droplet formation. *Am J Transl Res.* 2012; 4:102–113. [PubMed: 22347525]
32. Moran-Salvador E, Lopez-Parra M, Garcia-Alonso V, et al. Role for PPAR γ in obesity-induced hepatic steatosis as determined by hepatocyte- and macrophage-specific conditional knockouts. *FASEB J.* 2011; 25:2538–2550. [PubMed: 21507897]
33. Matsusue K, Haluzik M, Lambert G, et al. Liver-specific disruption of PPAR γ in leptin-deficient mice improves fatty liver but aggravates diabetic phenotypes. *J Clin Invest.* 2003; 111:737–747. [PubMed: 12618528]

34. Ratzu V, Charlotte F, Bernhardt C, et al. Long-term efficacy of rosiglitazone in nonalcoholic steatohepatitis: results of the fatty liver improvement by rosiglitazone therapy (FLIRT 2) extension trial. *Hepatology*. 2010; 51:445–453. [PubMed: 19877169]
35. Yu F, Su L, Ji S, et al. Inhibition of hepatic stellate cell activation and liver fibrosis by fat-specific protein 27. *Mol Cell Biochem*. 2012; 369:35–43. [PubMed: 22752386]

Author Manuscript

Author Manuscript

Author Manuscript

Author Manuscript

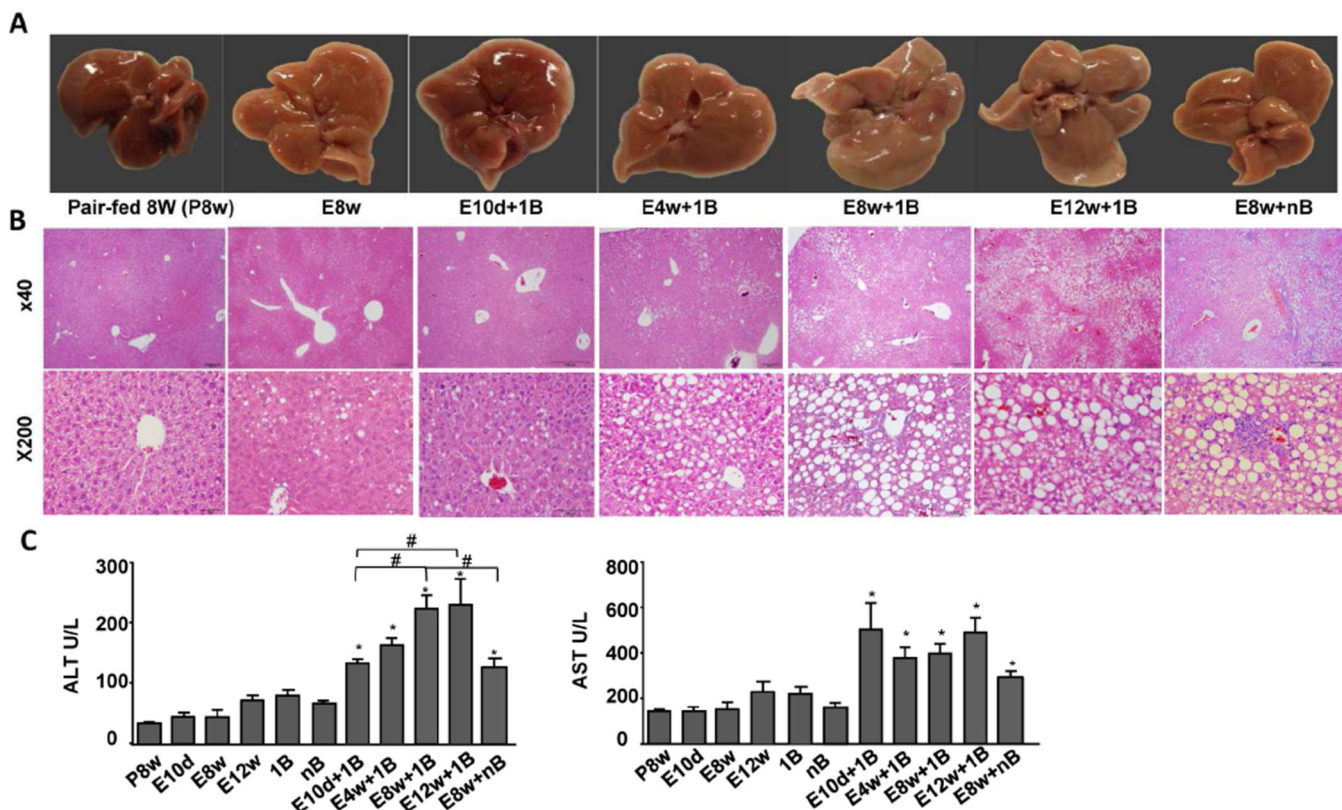


Figure 1. Chronic-plus-binge ethanol feeding induces ASH

A–C, Eight- to ten-week-old male C57BL6N mice were fed a liquid diet containing 5% ethanol for 10 days or for 4 to 12 weeks-plus-one binge (E10d+1B, E4-12w+1B) or with multiple binges (E8w+nB), for 8 weeks without a binge (E8w), or pair-fed (P8w); the mice were euthanized at 9 hours post-binge. (A) Representative images of livers. (B) Representative images of H&E staining. (C) Serum ALT and AST levels. Values represent the mean ± SEM (n=5–30 mice per group). **P*<0.05 in comparison with E8w; #*P*<0.05 as indicated.

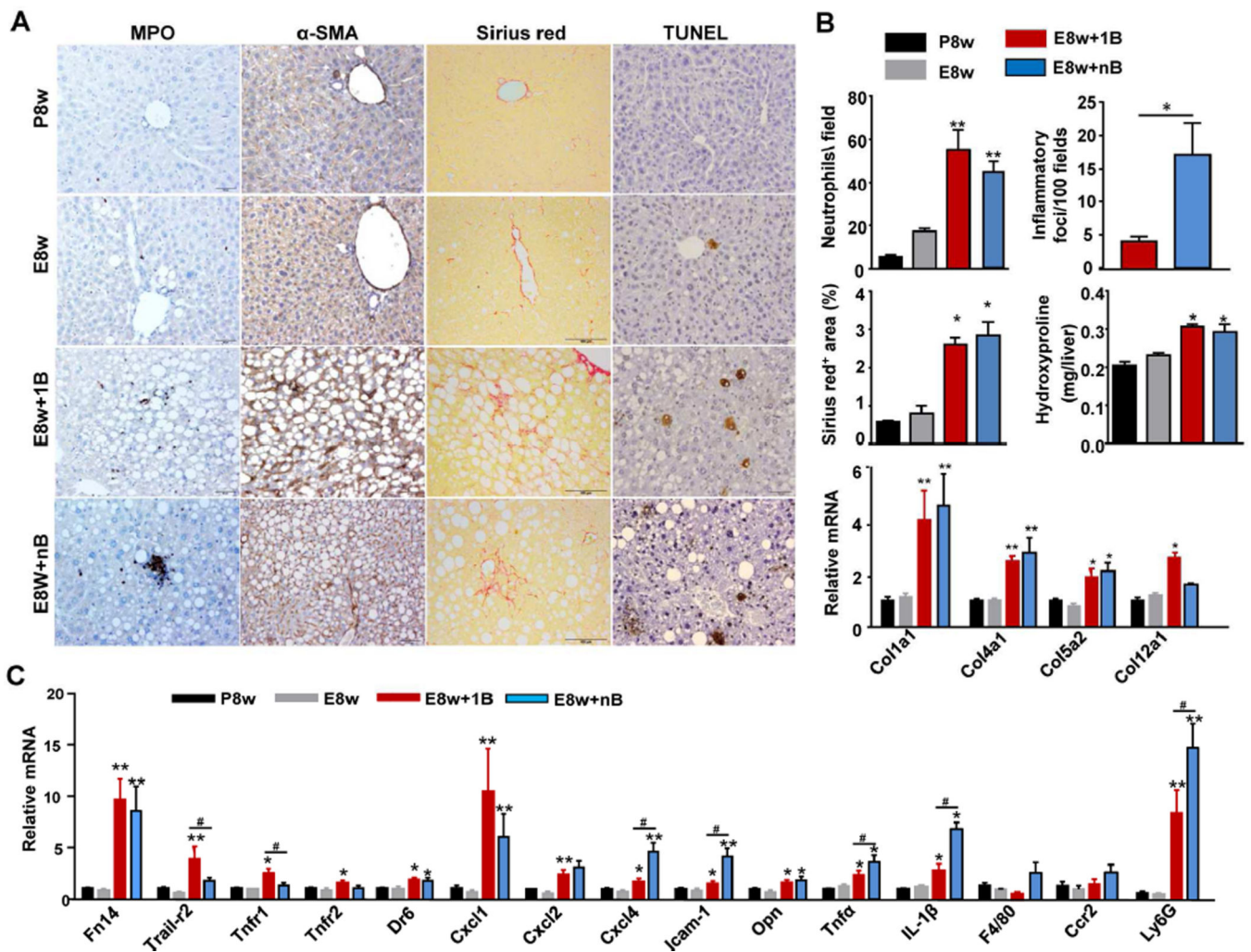


Figure 2. Characterization of chronic-plus-binge feeding model (E8w+1B and E8w+nB)
 (A) Representative photographs (200x) of various stainings of liver tissues. (B) Neutrophil infiltration per field (100x), number of inflammatory foci per 100 fields, Sirius red positive area, and hepatic expression of collagens were determined. (C) Real-time quantitative PCR analyses of pro-inflammatory genes. * $P < 0.05$, ** $P < 0.01$, *** $P < 0.001$ in E8w+1B and E8w+nB in comparison with P8w or E8w. # $P < 0.05$ as indicated. (n=5–8 mice per group).

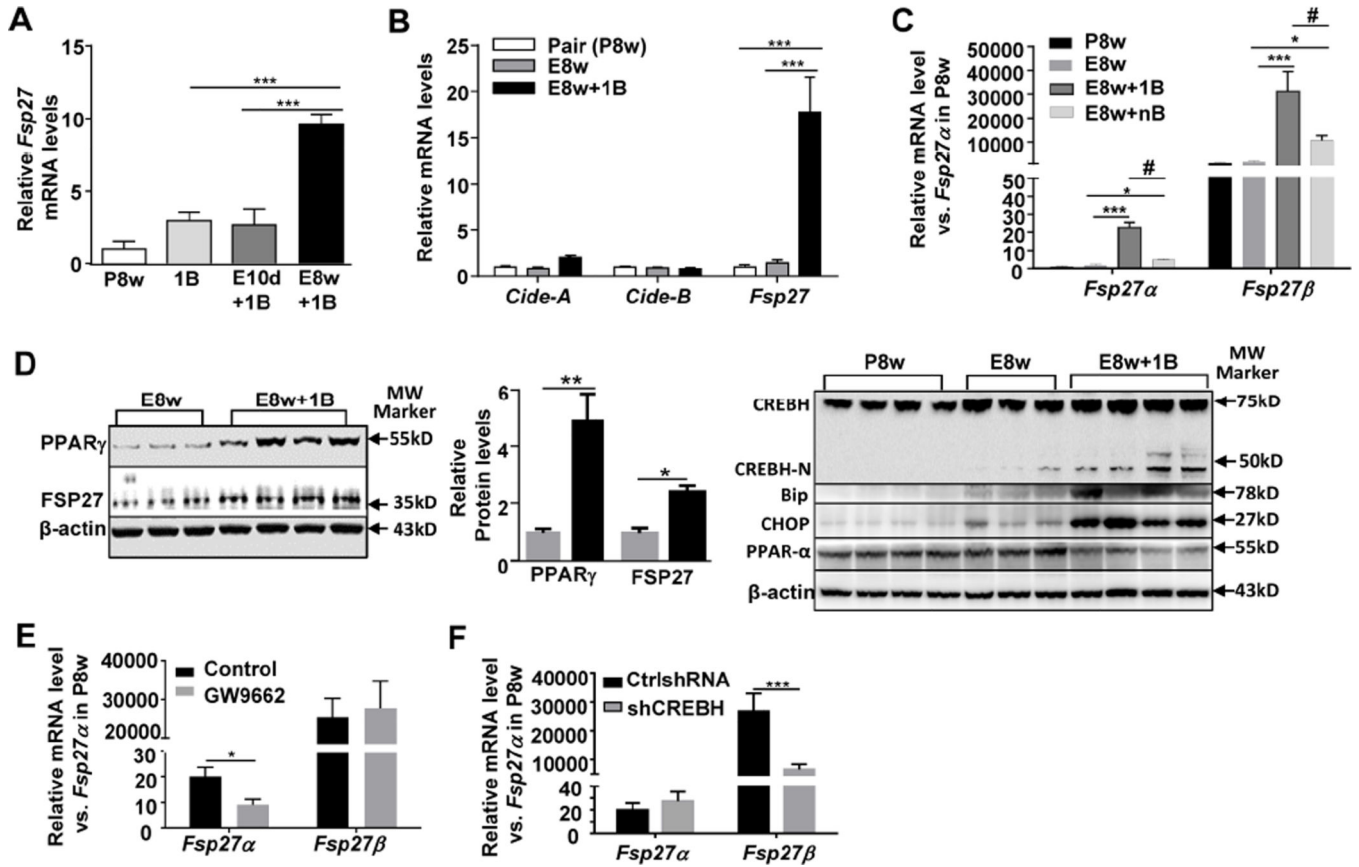


Figure 3. Chronic-plus-binge feeding upregulates hepatic *Fsp27α* and *Fsp27β* expression through PPAR γ - and CREBH-N-dependent mechanisms, respectively
Mice from different feeding models were used. (A, B, C) Real-time PCR analyses of liver tissues. (D) Western blot analyses of liver tissues. The density of the protein bands was quantified on the right panel. (E, F) Mice were fed E8w+1B, and vehicle or the PPAR γ inhibitor GW9662 was administered i.p. 15 minutes before the binge treatment, or infected with Ad-control-shRNA or Ad-shCREBH 5 days before ethanol gavage. Hepatic *Fsp27α* and *Fsp27β* mRNA levels were determined by real-time PCR analyses. * $P < 0.05$, ** $P < 0.01$, *** $P < 0.001$; # $P < 0.05$ as indicated. (n=3–12 mice per group).

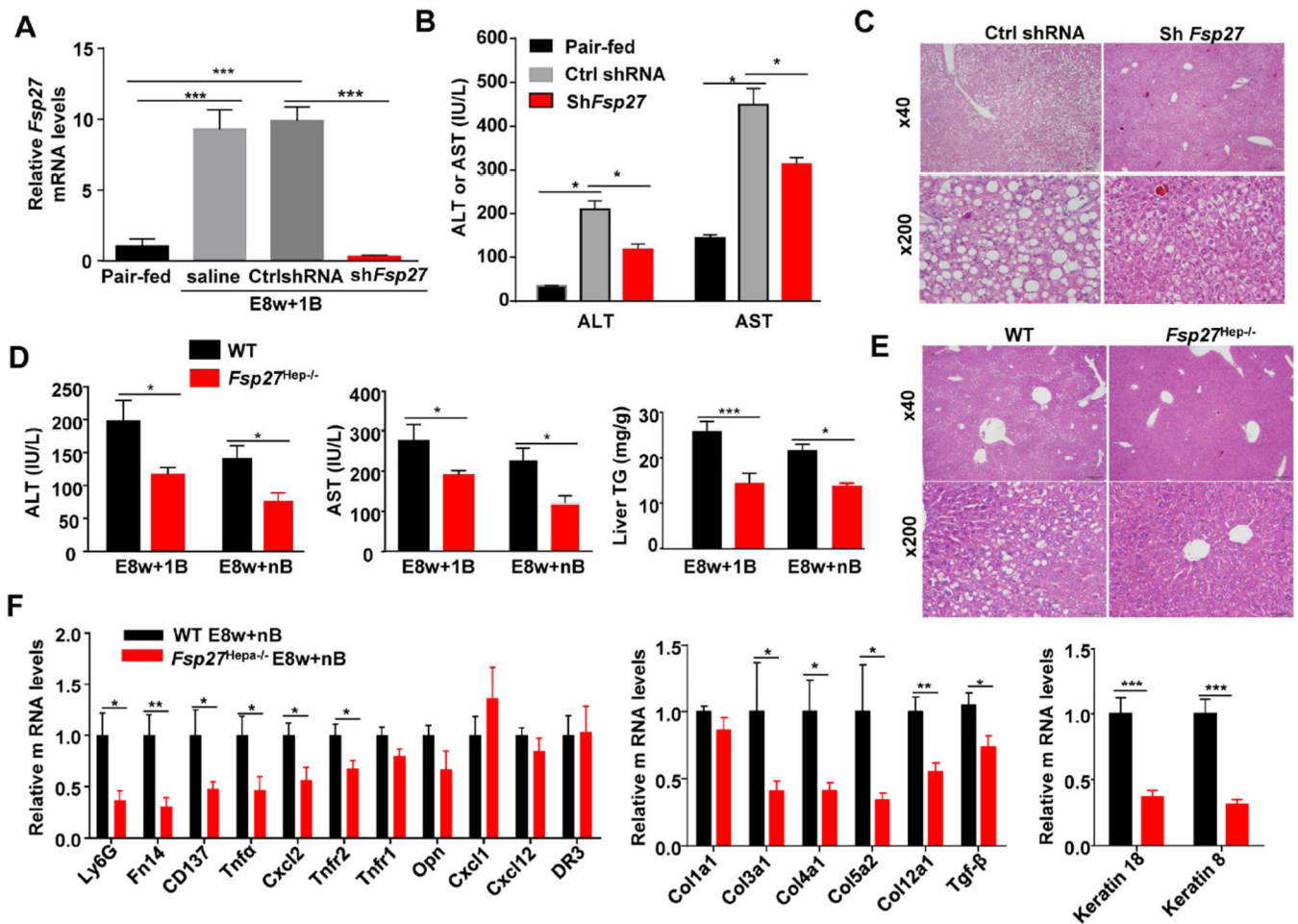


Figure 4. Inhibition of hepatic *Fsp27* ameliorates chronic-plus-binge ethanol-induced liver injury (A–C) Mice were fed E8w+1B and administered Ad-control-shRNA or Ad-sh*Fsp27* for the final 5 days. Real-time PCR analyses, serum ALT and AST levels, and representative H&E staining of the liver are shown. (D–F) *Fsp27^{Hep-/-}* and WT mice were fed E8w+1B or E8w+nB. Mice were euthanized 9 hours post the last binge. Serum ALT and AST levels, liver triglyceride levels, representative H&E staining (E8w+1B), and real-time PCR analyses are shown. **P*<0.05, ***P*<0.01, ****P*<0.001 as indicated. (n=6–8 mice per group).

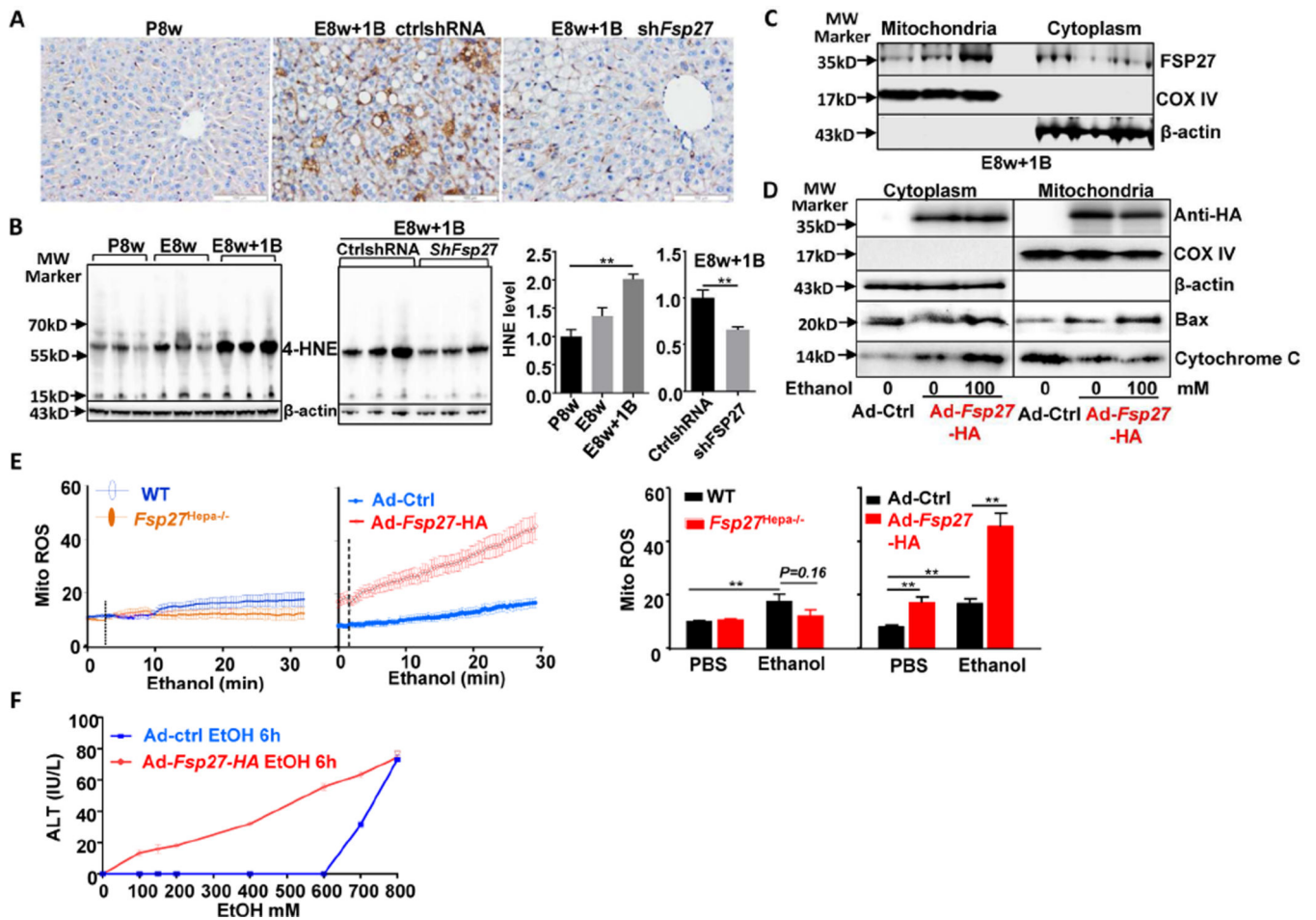


Figure 5. Ethanol and FSP27 synergistically induce mitochondrial ROS production and hepatocyte death

(A, B, C) Mice were fed E8w+1B and administered Ad-control-shRNA or Ad-shFsp27 for the final 5 days, and were euthanized 9 hours post binge. Liver tissues were subjected to MDA staining (panel A) and western blotting for 4-HNE (panel B). Cytoplasm and mitochondria were isolated from fresh liver tissues and subjected to western blot analysis (panel C). (D, E) Hepatocytes were infected with Adcontrol or Ad-Fsp27-HA for 36 hours, then incubated with ethanol for 6 hours. Cytoplasm and mitochondria were isolated for western blotting (panel D). Mitochondrial ROS generation was measured (panel E). ROS production was also measured in hepatocytes from WT and Fsp27^{Hep-/-} mice (panel E). (F) Ad-control-vector- or Ad-Fsp27-HA-treated hepatocytes were incubated with various concentrations of ethanol for 6 hours, ALT levels in the supernatant were measured.

* $P < 0.05$, ** $P < 0.01$.

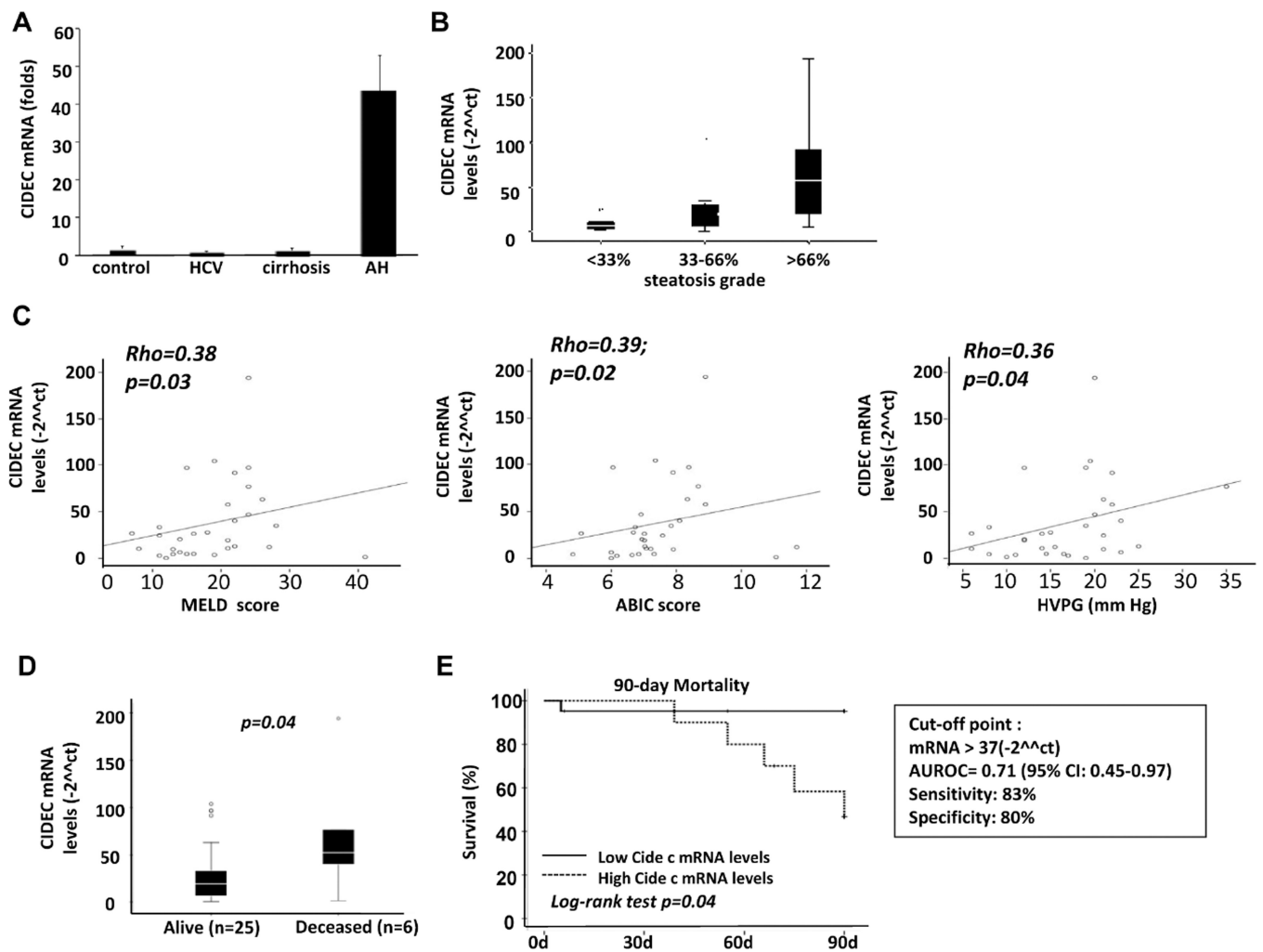


Figure 6. Hepatic *CIDEc* mRNA levels are increased and positively correlated with the severity of disease in AH patients
 (A) Real-time PCR analyses of liver samples from patients and from healthy controls. (B) Correlation between *CIDEc* mRNA and the degree of steatosis. (C) Correlation between *CIDEc* mRNA and MELD score, ABIC score, and HVPg. (D) Hepatic *CIDEc* mRNA levels in alive and deceased AH patients. (E) Hepatic *CIDEc* mRNA level and 90-day mortality. *P* values are presented in the figure.

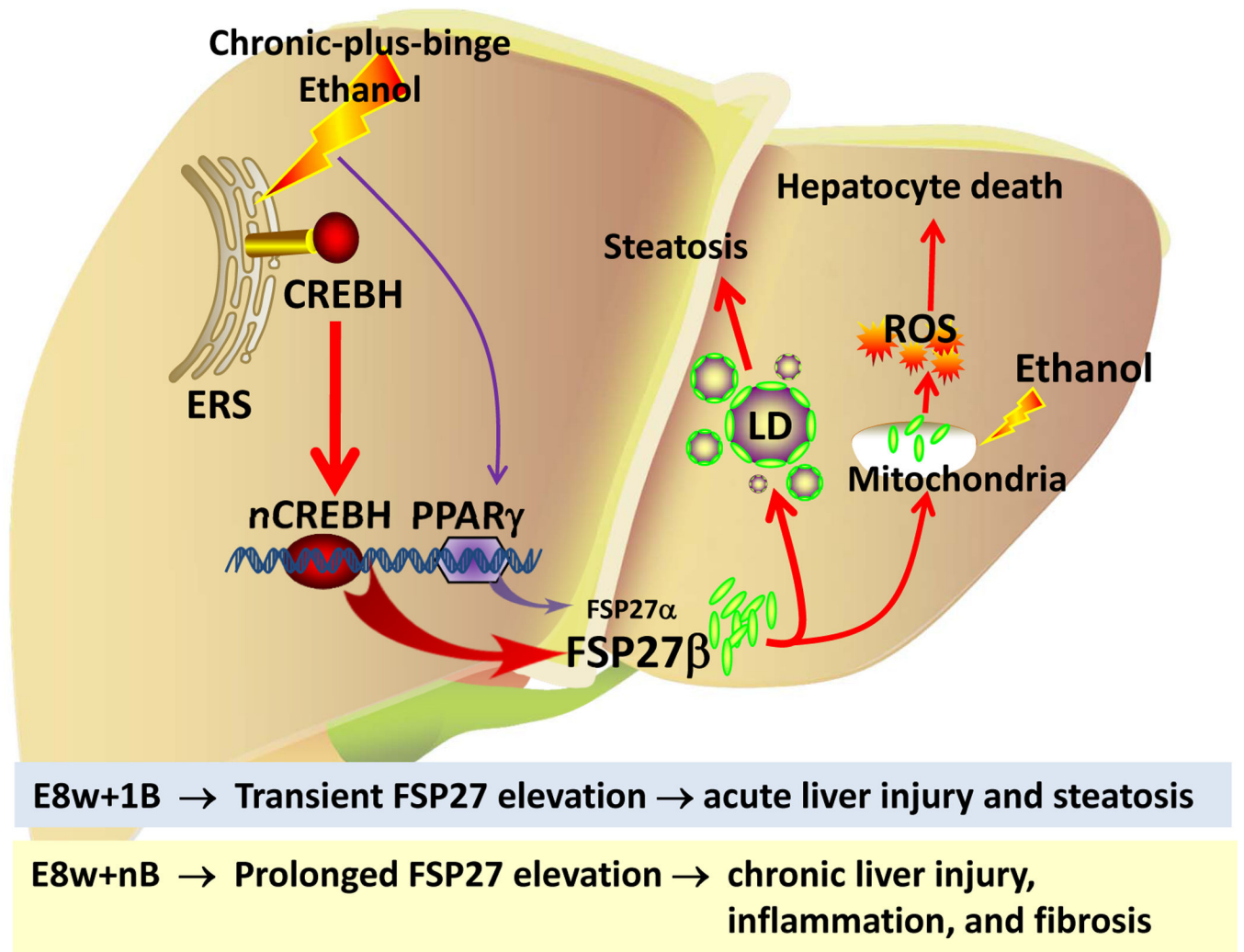


Figure 7. A proposed model for a critical role of FSP27 in chronic-plus-binge ethanol-induced ASH
 ERS: endoplasmic reticulum stress; LD: lipid droplet.